Optimization of Ligature/Bone Defect-Induced Periodontitis Model in Rats

Jingyi Gao
Southern Medical University
Simin Cai
Southern Medical University
Dan Li
Southern Medical University
Zijie Wang
Southern Medical University
Minyi Ou
Southern Medical University
Xinlu Zhang
Southern Medical University
Zhihui Tian (tianzh@i.smu.edu.cn)
Southern Medical University

Research Article

Keywords: periodontitis, animal model, bone defect, ligature, rat

Posted Date: September 20th, 2021

DOI: https://doi.org/10.21203/rs.3.rs-880589/v1

Abstract

Background

The destruction of alveolar bone is a crucial manifestation of severe periodontitis, which stem cell-based bioengineered therapies are expected to cure. Therefore, a cost-effective, reproducible, quantifiability and easier-to-administrate animal model that mimics human periodontitis is of great importance for further endeavor.

Methods

In this study, we created periodontitis rat models in silk ligation group, bone defect group and bone defect/silk ligation group respectively. he clinical indexes of periodontitis were observed and recorded. The mandible was taken for micro-computed tomographic, histological and histomorphometric analysis to assess the periodontal inflammation and bone remodeling

Results

Obvious periodontal inflammation but slight alveolar bone resorption were observed in the ligation group, while surgical trauma was not robust enough to continually worsen the constructed bone defect area in the bone defect group. In the bone defect/ligature group, obvious and stable periodontal inflammation could be the most lasting with similar evolving pathological patterns of human periodontitis. It also exhibited enhanced clinical similarity and confirmed its superiority in quantitativeness.

Conclusions

The present rat model is the first study to reproduce a pathological process similar to human periodontitis with reliable stability and repeatability, manifesting a priority to previous methods. Day 9 to Day 12 is the best time for reproducing severe periodontitis syndromes with vertical bone resorption in this model.

Background

Periodontitis is a chronic, multifactorial, infectious disease which can lead to the damage of periodontal tissues including gingiva, alveolar bone, cementum, periodontal ligament and even serious tooth loss (1). Worldwide epidemiological data show that a fraction of around 10% of those over 40–50 years in all populations exhibiting severe periodontitis (2). Periodontitis has become the prevalent cause of tooth loss in 90% of adults in the world today (3). It is also associated with systemic diseases such as heart disease, diabetes, Alzheimer's disease and pregnancy complications (4). At present, the mainstream clinical treatment of periodontitis is to control the development of periodontitis through initial therapy and periodontal surgery, but the ravaged periodontal tissue can seldom be restored (5). The regeneration of tissue loss caused by periodontitis is the ultimate goal of periodontal therapy (6). With the development of stem cells and bio-engineering, the research of periodontal regeneration therapy is making headway and it also points out the direction for the clinical treatment of

periodontitis (7). While the more promising periodontal tissue engineering treatment is still in the research stage, it is necessary to evaluate the effect of periodontal tissue regeneration through in vivo animal experiments.

Animal experiments are the indispensable pathways to evaluate any new treatments. At present, animal models used for the study of periodontal tissue regeneration are often created by bone defect modeling method, which establishes the acute bone defect by surgically removing part of the alveolar bone, periodontal ligament and cementum (6). Surgical creation of bone defects allows for rapid, stable, and quantifiable access to periodontal bone tissue for study (8). However, due to the lack of inflammatory microenvironment caused by accumulation of microbial plaque, the model obtained by acute bone defect is not satisfactory in etiology, development and prognosis of periodontitis (9, 10). The acute bone defects caused by surgery lack inflammatory induction process. Therefore, it is not widely used in periodontitis-related research (11). Instead, this method is more suitable for mechanical traumatic etiology (12, 13).

In order to overcome the shortcomings of bone defect modeling, some studies have combined the bone defect method with periodontitis silk ligation and successfully established periodontitis models of large animals (such as in miniature pigs and beagle dogs) (14, 15). Intraosseous defect is created on the alveolar bone and directly exposed to the oral environment(16), then the ligated silk threads are placed around the cervical region of the teeth to ensure long-term plaque deposition and accelerate the natural process of inflammation (17). This method not only ensures a more standardized morphology of the surgically created defect but also allows for reliable reproducibility of the study according to any given scheme, combining the rapid creation of periodontal bone tissue defects with the inflammatory microenvironment maintained by silk thread ligation method. It is a more appropriate model for the occurrence, development and prognosis of periodontal diseases in an inflammatory environment.

At present, there has been no report on the establishment of regenerative periodontitis model in rats by bone defect combined with silk ligature. In this regard, we proposed a novel surgical procedure to create bone defects in the mandibular molar region of rats by removing alveolar bone and tying the teeth with silk ligature. We observed and recorded the clinical manifestations of periodontitis. Micro-computed tomographic, histological and histomorphometric were also performed to analyze the inflammation and bone remodeling degrees. Our protocol have overcome the surgical operational obstacles of narrow oral region, small teeth of rats (18) and administrated reproducible and standardized bone defects in a rapider and greater manner. Afterwards, silk ligature was sutured around the cervical portion to simulate chronic periodontitis in rats. These optimizations are expected to better mimic the pathological process of periodontitis in both acute and chronic inflammation. We believe the present solution can facilitate the use of periodontitis models in periodontal regeneration research and shed light for the future study in the clinical effect of periodontal tissue regeneration therapy.

Methods

Establishment of animal model

Forty female SPF Wistar Rats, aging 8–12 weeks and weighing 220-240g (19), were obtained from the Animal Science Center of Southern Medical University (Guangzhou, China). Animals were acclimated for 1 week before periodontitis induction and they were housed under conventional condition with free access to water and food after periodontitis induction. Animal experiments were approved by the Institutional Review Board of the

Stomatological Hospital, Southern Medical University (201806) and by the Animal Care and Use Committees of Southern Medical University. Experimental procedures are all conformed to ethical principles of the revised Animals (Scientific Procedures) Act 1986. Rats were randomly divided into sham surgery group (only gingival incision and suture), ligature group (ligation of bilateral mandibular first molars), bone defect group (operation of buccal alveolar bone defect of bilateral mandibular molars) and bone defect/ligature group (operation of bilateral mandibular molars buccal alveolar bone defect and ligation of bilateral mandibular first molars) (Table 1). All rats were fasted for 24 hours. Weights were recorded and the anesthetic dosage were calculated according to body weight with 1% pentobarbital sodium (5ml/kg) injected intraperitoneally. The rats were fixed on the designed bed for rat dental surgery(previously Computer-aided designed and 3D printed in polylactic acid Fig. <link rid="fig1">1</link>A-1), and the tongue was pulled by the surgical silk thread to fully expose the visual field of the operation (Fig. 1A 2–3). The mucoperiosteal flap was raised and the alveolar bone was removed using surgical bur to create experimental periodontal defect between the mandibular first molar and second molar (Fig. 1B 1–4). The created alveolar bone defects were 1mm wide, 1mm long and 1mm deep (Fig. 1A 4–6). Subsequently, silk suture of the ligament was ligated around the cervical portion of the first molar and gingiva was intermittently sutured (Fig. 1B 5–6). Ligation and periodontal condition were checked every day. Rats were respectively sacrificed on days 3, 6, 9, 12, 15 and 18 after modeling (Fig. 1C). The body weight and vital signs such as heart rates and blood pressure were recorded before each rat was sacrificed in euthanasia using cervical dislocation under intraperitoneal injections of 1 mL of 75% ethanol.

Table 1
Groups division and respective surgical procedures

Group/Surgical procedures	Gingival flap elevation	Silk ligation	Surgical bone defect
Sham surgery	√		
Ligature		√	
Bone defect	√		√
Ligature + bone defect	√	√	√

Observation of clinical manifestations

To evaluate the degree of periodontitis, the probing depth, empyema, probing bleeding and loosening of the gingiva of the mandibular first molars of rats were measured with a CPI periodontal probe at each time point. Any inflammatory changes such as loss of gingival papilla, dislocation of gingival position or contour, redness, swelling and ulcer would be recorded. The periodontal pocket depths (PPD) in the buccal, mesial, distal and lingual sites of the mandibular first molars were respectively recorded with average values calculated. The Gingival Bleeding Index (GBI) (20) and the range of tooth mobility (TM) (21) of mandibular first molars are scored as previously described.

Micro-computed tomography (micro-CT) analysis

In order to observe alveolar bone loss at different time points and evaluate the effect of inflammation on bone tissue, the mandibles were fixed with paraformaldehyde. Micro-CT (Scano-Medical, Viva CTμ80, Switzerland) was used for computerized tomography and three-dimensional reconstruction. To assess alveolar bone loss, distances from the Cemento-Enamel Junction (CEJ) to the alveolar bone crest (ABC) were measured at four sites

of first molars (mesio-buccal, disto-buccal, mesio-palatal, and disto-palatal) in three-dimensional images viewed from buccal and palatal sides, with the assistance of the image analysis system RadiAnt Dicom Viewer (Medixant,Poland).Using the function of multi-plane reconstruction, the buccal-lingual cross section was set to the long axis of the distal root of the mandibular first molar, then the periodontal ligament widths were measured at apical 1/3, mid-root 1/3, and cervical 1/3. Images from different specimens were evaluated in a random sequence. The measurements were repeated two times per site.

Histomorphometric Analysis

In order to observe periodontal tissue inflammation and bone remodeling in rats, mandible was fixed with 10% paraformaldehyde, decalcified and embedded in paraffin. The tissue blocks were made into 5 μ m thick tissue sections through buccal and lingual direction, which were stained by hematoxylin-eosin (HE) and observed under a light microscope. To evaluate the degree of inflammatory cell aggregation and the integrity of alveolar bone and cementum, HE staining was visualized with confocal microscope (LSM 700, Carl Zeiss, Oberkochen, Germany). To observe the attachment loss, the Leica image analysis system was used to measure the distance from the cementum-enamel junction (CEJ) to the root of the junctional epithelium (50X) (11). The surgical area between the first and second molars was analyzed with 0–3 double-blind scoring system under light microscope(12). The sections of different specimens were evaluated according to random sequence and the measurements were repeated twice.

Statistical Analysis

Statistical analysis was performed using Statistical Package for the Social Sciences ver. 13 software (SPSS, Chicago, IL) and Graphpad Prism software (Graphpad, US). Data were representative of three or more independent experiments and all results were expressed as mean values ± standard deviation (SD), All data are subjected to Kolmogorov-Smirnov normality distribution testing and passed. Ranking data for GI and TM were evaluated Wilcoxon Rank sum test. Results were considered significant for $p < 0.05$. Quantitative data were evaluated by one sample t-test, one-way ANOVA and two-way ANOVA analysis, the $p < 0.05$ was considered statistically significant.

Results

Clinical manifestations

Weigh change in rats after periodontitis induction surgery is an important indicator for experimental safety and growth evaluation (22). Generally, all rats presented increase in their weights during the analysis period of 18 days (Fig. 2A). Differences of weight gain between four groups were not found to be statistically significant($p>0.05$). Rats of the bone defect plus ligation group lost about 2% of body weight on postoperative day 3, which may be due to the acute trauma and loss of blood, but they regained their initial body weight at day 6, confirming the ability to eat normally after surgery treatment. Statistical analysis indicated that no abnormalities were found both in blood pressure (Fig. 2B) and heart rate (data not shown) of all rats.

General status of the periodontal tissue was assessed by commonly-used clinical indexes including Bleeding Index (BI) (Fig. 2C) and Tooth Mobility (TM) (Fig. 2D). In terms of clinical indicators of periodontitis, the mean gingival bleeding index (BI) from 0–18 day postoperatively in the bone defect plus silk ligation group showed

significant differences from the remaining three groups (Fig. 2C, one sample t-test, $p < 0.0001$). Gingival bleeding by probing was more frequent in either the bone defect group or silk ligation group at the first day 3 to day 6. While gingival bleeding was more severe in the bone defect plus silk ligation group than in the rest of the groups from day 3 onwards, it was most severe and persistent at day 12–15 (Supplemental material 2).

For tooth mobility (TM), the bone defect plus silk ligation group had a significantly higher mean value of tooth loosening from 0–18 d postoperatively compared to either the bone defect or the silk ligation group (one sample t-test, $p < 0.0003$ for the bone defect group, $p < 0.0005$ for the wire group, and $p < 0.0001$ for the sham surgery group). Tooth mobility was highest in the bone defect group on day 6, and reached its peak on days 9–12 in both the silk ligature group and the bone defect/silk ligature group (Supplemental material 2).

Morphometry of Micro-CT images

Micro-CT is a very sensitive technique for displaying hard tissue conditions and providing three-dimensional images. Correlation between reconstructions by three-dimensional micro-CT images and histomorphological metrics of periodontitis models has been demonstrated (11). Therefore, to evaluate periodontal condition, we used micro-CT to measure periodontal ligament width and alveolar bone loss.

Our results manifested a smooth alveolar bone cortex in the sham surgery group during 6–18 days and only mild horizontal resorption of alveolar bone was observed (Supplemental material 2). There was no significant widening of the periodontal ligament in the sham group during the 18 days (Fig. 3A 4–6, mean = 0.307, SD = 0.024).

As for the ligature group, during the first nine days, the alveolar bones cortex was partially dissolved. From day nine onwards, fractured cortical bone on the alveolar bone surface and sparse cancellous bone trabecular structures were observed. Mild horizontal resorption with progressive and irregular bone loss pattern was observed on day 12–18 (Fig. 3A 8–9). Periodontal ligament width changed mildly, peaking at 9 day and later with a slight decrease are observed in the silk ligature group on Day 18 (Fig. 3A 10–12).

In the bone defect group, the surgical alveolar bone defect between the area of the first and second molar bone was clearly detected (Fig. 3A 13). The depth of the bone defect area slightly increased and restorative tissue was formed at the edge of the area from 12 day onwards (Fig. 3A 14). The bone defect was partially restored after 18 days (Fig. 3A 15). Slight increase of periodontal ligament in the bone defect group was witnessed from 6 days postoperatively (Fig. 3A 16) and a gradual decrease from 12 to 18 days (Fig. 3A 17–18).

In the bone defect/ligation group, rough surface of the alveolar bone, typical horizontal and vertical resorption were obvious six days after surgery (Fig. 3A 19). Meanwhile, the surgical defect area remains a relatively identifiable contour. A rapid increase of CEJ-ABC distance in the bone defect/ligature group occurred from day 3 to day 6 (Fig. 3A 19), peaking at 9–12 day (Fig. 3A 20) and followed by a gradual decrease from day 15–18 (Fig. 3A 21). In bone defect/ligature group, PDL width increased rapidly in 6 day onwards (Fig. 3A 22), reaching at highest in the day 9 and decreased gradually afterwards (Fig. 3A 23–24). Still, it remains significantly higher than that in the rest groups during the whole period of 6-18d (Fig. 3C). Overall, the amount of alveolar bone resorption established by bone defect combined with silk ligation was significantly higher than the remaining three groups (Fig. 3B, one sample t-test, $p < 0.0001$), with a most active inflammation of periodontitis maintaining the longest time period (Fig. 3D).

Histological analysis

Histopathologic assessment is the golden criterion for periodontal healing and regeneration in animal models of periodontitis. The evaluation of the central portion of the surgical site of the bone defect yields representative histometric data (15). The depth of the periodontal pockets was measured on the HE sections (Fig. 4A & Fig. 3E). The level of attachment loss was determined by measuring the distance from the CEJ to the apical extent of the attached epithelium (Fig. 4A). In the present study, we also set up a double-blind scoring system based on the degree of the infiltration of inflammatory cells in sucular epithelium, gingival connective tissues, alveolar bone loss, periodontal ligaments continuity, Sharpey's fibers completeness in the position of the distal root of the mandibular first molar (Fig. 3D).

The primary clinical change observed in the rats in the bone defect/ligation group from day 3 onwards was the appearance of reddish hyperemia and shiny acute edema. Pathologically, the proliferated capillaries and capillary loops can be witnessed near the sucular epithelium with emerged PMNs and destructed collagen. As expected, the periodontal pocket depth in the bone defect group maintained at a low level during the first 6 days after surgery (Fig. 3E). No significant difference of gingival soft tissue inflammation was found compared to the sham surgery group (Fig. 3D), indicating that the bone defect surgery alone does not cause persistent irritation of the periodontal ligament. There was a distinct mechanical defect area in the buccal alveolar ridge in bone defect group with blood clot and osteoblasts observed on the Day six due to the initiation of bone healing process.

In the silk ligation group, histological ravage of normal color and contour of the gingival tissue was observed from Day 9 onwards (Fig. S1). Loose gingival tissue and disconnected apical periodontal ligament could be witnessed due to the continuously plaque accumulation but the inflammation infiltration was not severe and the resorption in cortical bone was uneven. The ligature group did not produce deep periodontal pockets until nine days after surgery (Fig. 3E). In bone defect group, initial osteogenesis of the surgical area was observed with fibrous new bone formation. Meanwhile, in the bone defect/ligature group during Day 9–12 a large number of inflammatory cells infiltrated and ulcerated in the periodontal pockets as the lesion progressed (Fig. 4B 13). Polymorphonuclear leukocytes appeared under the crevicular epithelium and penetrated the junctional epithelium into the gingival sulcus. Periodontal pockets deepened when the epithelial attachments moved along the root surface apically leading to loss of attachment. Macrophages appeared under the affected epithelium and the junctional epithelium was detached from the tooth surface, at which point the inflammation reached its peak (Fig. 4B 14).

On the 15–18 days after the surgery, infiltration of inflammatory cells was no longer found in the bone defect group. The repaired alveolar bone was still cortically spongy but the defected triangle-shaped alveolar crest was already flattened. Due to the gradual immune adaption of bacteria, the ligature group manifested a tendency of rapid decreasing of acute inflammation after Day 15. The subsided inflammation at the gingival margin and relieved shallowing of the PD were witnessed (Fig. S1). Acute inflammation in the bone defect/ligature group also decreased slowly after Day 15 but still remained significantly higher from the other groups till Day 18 (Fig. 3D). The PDL width gradually decreased in the later stage in bone defect/ligation group (Fig. 3C), while the height of the defect alveolar bone was less regenerated than that in the bone defect group (Fig. 3B).

Discussion

A variety of methods have been proposed by different studies to induce experimental animal models of periodontitis (23). It is generally believed that periodontitis animal models should represent the obvious processes of plaque attachment, gingival inflammation, attachment loss and alveolar bone loss observed in human disease (24). For these reasons, we choose to induce animal model by alveolar bone removal surgery in association with ligature placement. We successfully reduced the obstacles of fixing rat's body position and exposing the surgical region in the narrow oral cavity by designing a customized dental surgery bed (Fig. 1A 1–3). Overall, the application of our process can effectively improve the efficiency of periodontitis modeling in rats (the average successful rate is 82.6%, data not shown).

Periodontitis is a chronic inflammatory response that results from the interaction between the host immune system and oral pathogens(12). That's why previous experimental studies generally used models that resulted from plaque accumulation which gradually induce periodontitis. However, the induction period of such approach takes longer than 5–7 months to develop primary clinical gingivitis in dogs(15). In our study, the maximum peak periodontitis was obtained as early as the 9th day (Fig. 3B-E). Animals such as monkeys, miniature pigs and beagle dogs are seldom the first choice for periodontium regeneration research because they are expensive to culture and require a high standard for experimental equipment (25). The breeding and housing costs of rodent animals are relatively low, making it possible to carry out studies with sufficient mass for statistical analysis (26). Rat modeling was therefore faster, easier and more cost-effective. Nowadays, gene knockout rats have been widely cultured in recent years especially for the study of the specific roles of genes in regulating pathological process, inflammation responses and tissue regeneration of periodontitis. A large number of studies have used genetically-engineered rats to study the underlying mechanism of systemic inflammation and its effect on periodontal healing. Rats can be ideal animals for the study of periodontal diseases, which are suitable not only for the study of teeth, but also for the dynamic interaction of soft-hard tissue related to oral inflammation (26).

Meanwhile, previous study found that ligature alone did not induce stable and lasting periodontal bone loss in rats, as the regression of inflammation and the healing of alveolar bone were too observed in the ligature group of our study from Day 12 to Day 18 (Fig. 3A 8–9). The decrease of CEJ-ABC was also rather random in individual rat, making it difficult to achieve standardized measurement for comparable data analysis. Therefore, we also optimized the surgical bone removal protocol in rats according to pre-described anatomical landmarks (Fig. 1A 4–6). The 3D micro-CT reconstructed images of the mandibular first and second molars showed similar triangular area of bone defect after operation, which proved that the operation location was reliably repeatable (Fig. 3A 13&19). The method proposed in this study not only produces a standardized morphological defect area, but also ensures reliable data for repetitive comparison research according to any given scheme. For an instance, any amount of regenerative osseous tissue provoked by certain regenerative periodontal treatment (manifesting as a blurring margin and the shallowing of the triangle surgical defect, Fig. 1D) might be easily identified, measured and quantitated. Compared to the mainstream ligation method, the model we induced manifest a significantly faster progression, longer duration and a more standardized bone absorption area of experimental periodontitis during the same period. Therefore, we believed that the present established a model of periodontitis in rats by alveolar bone defect in association with silk ligature confirmed its superiority to

previous methods, proving its essentiality to be a suitable experimental model for regenerative periodontal treatment evaluation.

By far, no satisfying model similar to the pathologic process of human periodontitis has been proposed (23). In present study, we obtained various methods to evaluate the model outcomes of periodontitis at different time points, including the two-dimensional CT panel of labial-lingual section, the micro-CT reconstructed three-dimensional model and HE stained histopathological sections, all reporting obvious time-pattern changes and specificity. The present rat models we established, induced by acute alveolar bone defect and chronic silk ligature, is the first to successfully mimic the pathological changes in periodontal tissue and stages divisions in human periodontitis (Table 2).

Table 2
Differences of stages of gingivitis and periodontitis between humans and rats

Stage	Humans			Rats		
	Time (days)	Clinical Findings	Underlying microscopical features	Time (days)	Clinical Findings	Underlying microscopical features
.Initial lesion	2–4	• Gingival fluid flow	• Vascular dilation • Infiltration by PMNs • Perivascular collagen loss	0–3	• NOT clinically evident • subclinical gingivitis	• gingival vasculature • PMNs exudation • fibrin deposition
.Early lesion	6–8	• Erythema Bleeding on probing	• Vascular proliferation • Lymphocytes infiltration • Increased collagen loss around infiltrate	3–6	• erythema of the gingival margin • “marginal gingivitis”	• PMNs into pocket area • collagen destruction • proliferated capillaries and capillary loops
.Established lesion	14–21	• Changes in color, size, texture, and so on	• Vascular proliferation and blood stasis • Plasma cells infiltration • Continued loss of collagen	6–9	• bluish tinge may become superimposed on the reddened gingiva (anoxemia) • gingival edema	• plasma cells increase • widened intracellular spaces with PMNs • congested vessels • RBCs extravasate
. Advanced lesion	>28	• consistent bleeding (gingival index = 2) • more attachment loss	• fibrosis of the gingiva • widespread tissue damage • plasma cells and neutrophils dominating epithelium	9–12	• probing bleeding • pocket form • attachment loss	• slight alveolar bone loss

Stage	Humans			Rats		
	Time (days)	Clinical Findings	Underlying microscopical features	Time (days)	Clinical Findings	Underlying microscopical features
.periodontitis	For years	• plaque and calculus, gingival swelling, redness • Deep PDD • BOP(+) • Attachment and bone loss (angular/vertical or horizontal) • Increased tooth mobility	• Degeneration and inflammatory exudate • edema • inflamed engorged connective tissue, expanding rete pegs	15–18 onwards	• oral inflammatory changes (erythema, edema, hemorrhage) intensify • horizontal and vertical (or angular) bone loss • Increased tooth mobility	• alveolar bone is lost via osteoclastic activity

At day 3, experimental region between the mandibular first and second molars of rats showed clear-cut triangular bone defect area (Fig. S1). Mild hyperemia of blood vessels was observed in the gingival tissues with low clinical indexes of BI and TM (Fig. 2C&D), indicating that ligation hadn't led to obvious plaque accumulation yet. This stage can be regarded as the initial lesions of human periodontitis, showing similarity in clinical manifestations and pathological progress (27). In 6–9 days, the activity of periodontitis increased due to plaque accumulation, initiating inflammatory cell infiltration. As more of the gingiva becomes affected, bleeding may be spontaneous as the clinical manifestations of marginal gingivitis (28) (Fig. S1). Rough surface of alveolar bone was captured both by micro-CT and histopathologic sections, corresponding to the early lesions of human periodontitis (Fig. 3A 19). With the progress of the experiment, the destruction of periodontal tissue exacerbated (Fig. 4A and Fig. S1) in the Day 9 to 12 (Fig. 4B 13). The connection between the junctional epithelium and the dentin surface was greatly loose with polymorphonuclear leukocytes (PMNs) infiltration. The connective tissue showed significant RBC extravasation and collagen fibers disappearance (Fig. 4B 14). In our study, bone loss peaked at 9 days postoperatively (Fig. 3B). Significant horizontal and vertical bone resorption was formed causing the height of alveolar crest decreased, and the loss of buccal bone reached more than 1/2 (Fig. 3A 20&23). By far, the expression of periodontal tissue is close to the clinical manifestations of the established stage in human periodontitis. From 15 to 18 days, the acute gingival inflammation was slightly alleviated (Fig. S1). This may be a result of the conversion of the innate responses of the rat immune system to adaptive responses to produce protection of periodontal tissue, but at this point the reduced alveolar bone height is not significantly recovered and chronic periodontal destruction will persist (Fig. 3A 21). Periodontal loss is considered to be irreversible, meaning that lost bone cannot be regained without advanced regenerative surgeries(29). Therefore, the optimal experimental period of our model is from 9 to 12 days.

Conclusion

In summary, having integrated the advantages of both acute bone defect and chronic silk ligature methods, our rat model better represent the evolving process of human periodontitis, showing a great similarity between rats

and humans in the divisions of clinical syndromes and pathological changes (27). It can be fully applied to the study during the period of Day 9–12 when reaches the most active peak. Present protocol proves to establish a suitable experimental model for the regenerative research of periodontitis, as the stability and reproducibility of alveolar bone resorption triumphs over the rest of the methods as demonstrated above. The optimization of this model is anticipated to contribute to the application of periodontitis animal model in the future research, especially in the evaluation of clinical efficacy as well as the underlying mechanism of periodontal regeneration therapy.

Declarations

Ethics approval and consent to participate

Animal experiments were approved by the Institutional Review Board of the Stomatological Hospital, Southern Medical University (201806) and by the Animal Care and Use Committees of Southern Medical University. Experimental procedures are all conformed to ethical principles of the revised Animals (Scientific Procedures) Act 1986. The study was carried out in compliance with the ARRIVE guidelines.

Consent for publication

Not applicable.

Availability of data and materials

The datasets used and/or analysed during the current study are available from the corresponding author on reasonable request.

Competing interest

All authors report no competing interest for this paper.

Authors' contributions

All authors have made substantial contributions to conception and design, establishment of animal model, analysis or interpretation of data in this study. Jinyi Gao carried out histomorphometric analysis, observation of clinical index and drafted the manuscript. Simin Cai carried out micro-CT analysis and participated in observation of clinical index, all data analysis and manuscript drafting. Minyi Ou participated in the study design and the data analysis, helped to perform the tissue sample preparation and revise the manuscript. Dan Li performed the tissue sample preparation, participated in the data analysis and advised on the study design. Zijie Wang advised on the data analysis and helped to revise the manuscript. Xinlu Zhang advised on the data analysis and reviewed the manuscript. Zhihui Tian conceived of the study, carried out the study design, helped to draft and revise the manuscript. All authors read and approved the final manuscript.

Funding

This work was supported by the National Natural Science Foundation of China [818003710], Foundation of President of Nanfang Hospital [grant.MO 2018B014] and GuangDong Basic and Applied Basic Research

Foundation [2021A1515011656]. This work was also supported by grants from Guangdong Basic and Applied Basic Research Fund Project [Grant No.2019A1515011503, to YGT].

Acknowledgments

We thank Dr. Xujia Lai, for her review and technical support for the statistical analysis in this paper.

References

1. Bouchard P, Carra MC, Boillot A, Mora F, Range H. Risk factors in periodontology: a conceptual framework. J Clin Periodontol. 2017;44(2):125-31.
2. Eke PI, Dye BA, Wei L, Slade GD, Thornton-Evans GO, Borgnakke WS, et al. Update on Prevalence of Periodontitis in Adults in the United States: NHANES 2009 to 2012. J Periodontol. 2015;86(5):611-22.
3. Nibali L, Farias BC, Vajgel A, Tu YK, Donos N. Tooth loss in aggressive periodontitis: a systematic review. J Dent Res. 2013;92(10):868-75.
4. Hayashi K, Hasegawa Y, Takemoto Y, Cao C, Takeya H, Komohara Y, et al. Continuous intracerebroventricular injection of Porphyromonas gingivalis lipopolysaccharide induces systemic organ dysfunction in a mouse model of Alzheimer's disease. Exp Gerontol. 2019;120:1-5.
5. Trofin EA, Monsarrat P, Kemoun P. Cell therapy of periodontium: from animal to human? Front Physiol. 2013;4:325.
6. Petersen A, Princ A, Korus G, Ellinghaus A, Leemhuis H, Herrera A, et al. A biomaterial with a channel-like pore architecture induces endochondral healing of bone defects. Nat Commun. 2018;9(1):4430.
7. Pellegrini G, Seol YJ, Gruber R, Giannobile WV. Pre-clinical models for oral and periodontal reconstructive therapies. J Dent Res. 2009;88(12):1065-76.
8. Shujaa Addin A, Akizuki T, Matsuura T, Hoshi S, Ikawa T, Maruyama K, et al. Histological healing after nonsurgical periodontal treatment with enamel matrix derivatives in canine experimental periodontitis. Odontology. 2018;106(3):289-96.
9. Fawzy El-Sayed KM, Dorfer CE. (*) Animal Models for Periodontal Tissue Engineering: A Knowledge-Generating Process. Tissue Eng Part C Methods. 2017;23(12):900-25.
10. Finger Stadler A, Patel M, Pacholczyk R, Cutler CW, Arce RM. Long-term sustainable dendritic cell-specific depletion murine model for periodontitis research. J Immunol Methods. 2017;449:7-14.
11. Li CH, Amar S. Morphometric, histomorphometric, and microcomputed tomographic analysis of periodontal inflammatory lesions in a murine model. J Periodontol. 2007;78(6):1120-8.
12. Xie R, Kuijpers-Jagtman AM, Maltha JC. Inflammatory responses in two commonly used rat models for experimental tooth movement: comparison with ligature-induced periodontitis. Arch Oral Biol. 2011;56(2):159-67.
13. Batool F, Strub M, Petit C, Bugueno IM, Bornert F, Clauss F, et al. Periodontal Tissues, Maxillary Jaw Bone, and Tooth Regeneration Approaches: From Animal Models Analyses to Clinical Applications. Nanomaterials (Basel). 2018;8(5).
14. Liu Y, Zheng Y, Ding G, Fang D, Zhang C, Bartold PM, et al. Periodontal ligament stem cell-mediated treatment for periodontitis in miniature swine. Stem Cells. 2008;26(4):1065-73.

15. Koo KT, Polimeni G, Albandar JM, Wikesjo UM. Periodontal repair in dogs: analysis of histometric assessments in the supraalveolar periodontal defect model. J Periodontol. 2004;75(12):1688-93.
16. Wang S, Liu Y, Fang D, Shi S. The miniature pig: a useful large animal model for dental and orofacial research. Oral Dis. 2007;13(6):530-7.
17. Vargas-Sanchez PK, Moro MG, Santos FAD, Anbinder AL, Kreich E, Moraes RM, et al. Agreement, correlation, and kinetics of the alveolar bone-loss measurement methodologies in a ligature-induced periodontitis animal model. J Appl Oral Sci. 2017;25(5):490-7.
18. Kim SE, Lee ER, Lee Y, Jeong M, Park YW, Ahn JS, et al. A modified method for inducing periodontitis in dogs using a silk-wire twisted ligature. J Vet Sci. 2012;13(2):193-7.
19. Duan X, Gleason RC, Li F, Hosur KB, Duan X, Huang D, et al. Sex dimorphism in periodontitis in animal models. J Periodontal Res. 2016;51(2):196-202.
20. da Silva FRP, M ESCP, de Carvalho Franca LF, Alves EHP, Dos Santos Carvalho J, Di Lenardo D, et al. Sulfated polysaccharides from the marine algae Gracilaria caudata prevent tissue damage caused by ligature-induced periodontitis. Int J Biol Macromol. 2019;132:1-8.
21. Xu Y, Wei W. A comparative study of systemic subantimicrobial and topical treatment of minocycline in experimental periodontitis of rats. Arch Oral Biol. 2006;51(9):794-803.
22. Yu T, Zhao L, Huang X, Xie M, Wang X, Ma C, et al. Postoperative Weight Loss Masks Metabolic Impacts of Periodontitis in Obese Rodents. J Periodontol. 2017;88(6):e97-e108.
23. Donos N, Park JC, Vajgel A, de Carvalho Farias B, Dereka X. Description of the periodontal pocket in preclinical models: limitations and considerations. Periodontol 2000. 2018;76(1):16-34.
24. Graves DT, Correa JD, Silva TA. The Oral Microbiota Is Modified by Systemic Diseases. J Dent Res. 2019;98(2):148-56.
25. Chiu HC, Chiang CY, Tu HP, Wikesjo UM, Susin C, Fu E. Effects of bone morphogenetic protein-6 on periodontal wound healing/regeneration in supraalveolar periodontal defects in dogs. J Clin Periodontol. 2013;40(6):624-30.
26. Kantarci A, Hasturk H, Van Dyke TE. Animal models for periodontal regeneration and peri-implant responses. Periodontol 2000. 2015;68(1):66-82.
27. Takata T, Donath K. The mechanism of pocket formation. A light microscopic study on undecalcified human material. J Periodontol. 1988;59(4):215-21.
28. Page RC SH. Periodontitis in man and animals. A comparative review. Basel: Karger. 1982.
29. Dahlen G, Fejerskov O, Manji F. Current concepts and an alternative perspective on periodontal disease. BMC Oral Health. 2020;20(1):235.

Figures

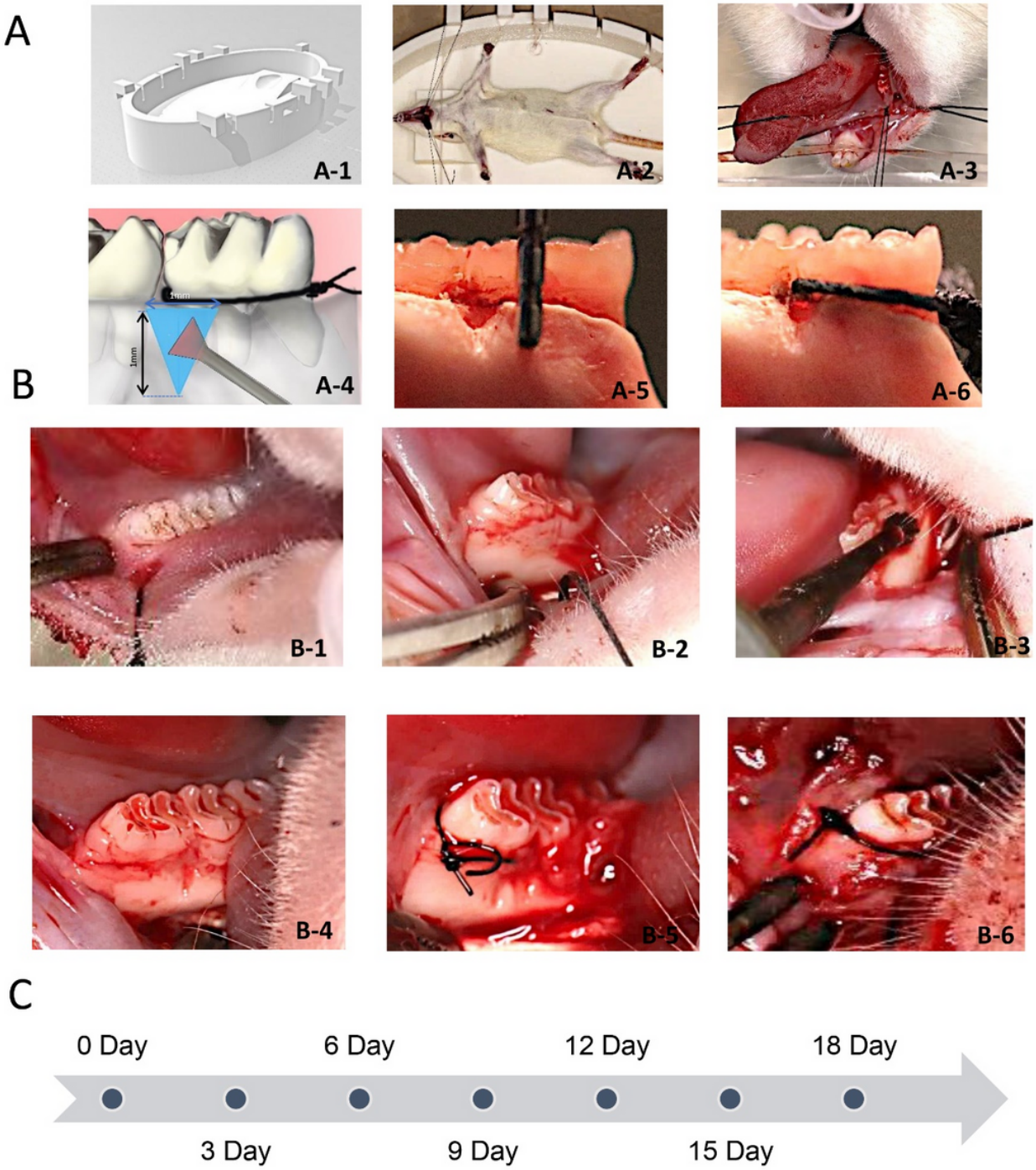

Figure 1

The establishment of rat periodontitis model by bone defect combined with silk ligation. A: (A1-A3)design and application of rat dental operation bed: A-1 3D modeling of rat dental operation bed; (A-2) operation position and fixation method; (A-3) suture traction to expose oral operation field. A4-A6 Schematic diagram of bone defect and silk thread ligation: (A-4) standardized manufacture of bone defect (the experimental region is shown in the blue triangle). The anatomical location of triangular bone defect as follows: 1. The long axis of the parallel tooth between the first molar and the second molar to the starting point of the oblique line. The midpoint of the buccal side of the first molar to the starting point of the outer oblique line 3. The buccal midline of the first

molars is between the first molars and the second molars;A-5the measurement of bone defect area by graduated periodontal probe (A-6) the ligated silk thread is closely attached to the cervical portion of the mandibular first molars. B: operation steps: (B-1): Exposure of the operative field on the rat dental surgical bed. (B-2) Exposure of the mandible by gingival flap on the buccal side of the mandibular first and second molars. (B-3) Removal of bone tissue from the operative area of the bone defect by the dental slow speed bur. (B-4) rinsing and hemostasis of the operative area. (B-5) Ligation of 5-0 sutures on the cervical part of the first molar in rats. (B-6) the overall appearance of oral cavity after primary suture of free gingival flap. C: Timeline: the rats were sacrificed and samples were taken on the 3rd, 6th, 9th, 12th, 15th and 18th day.

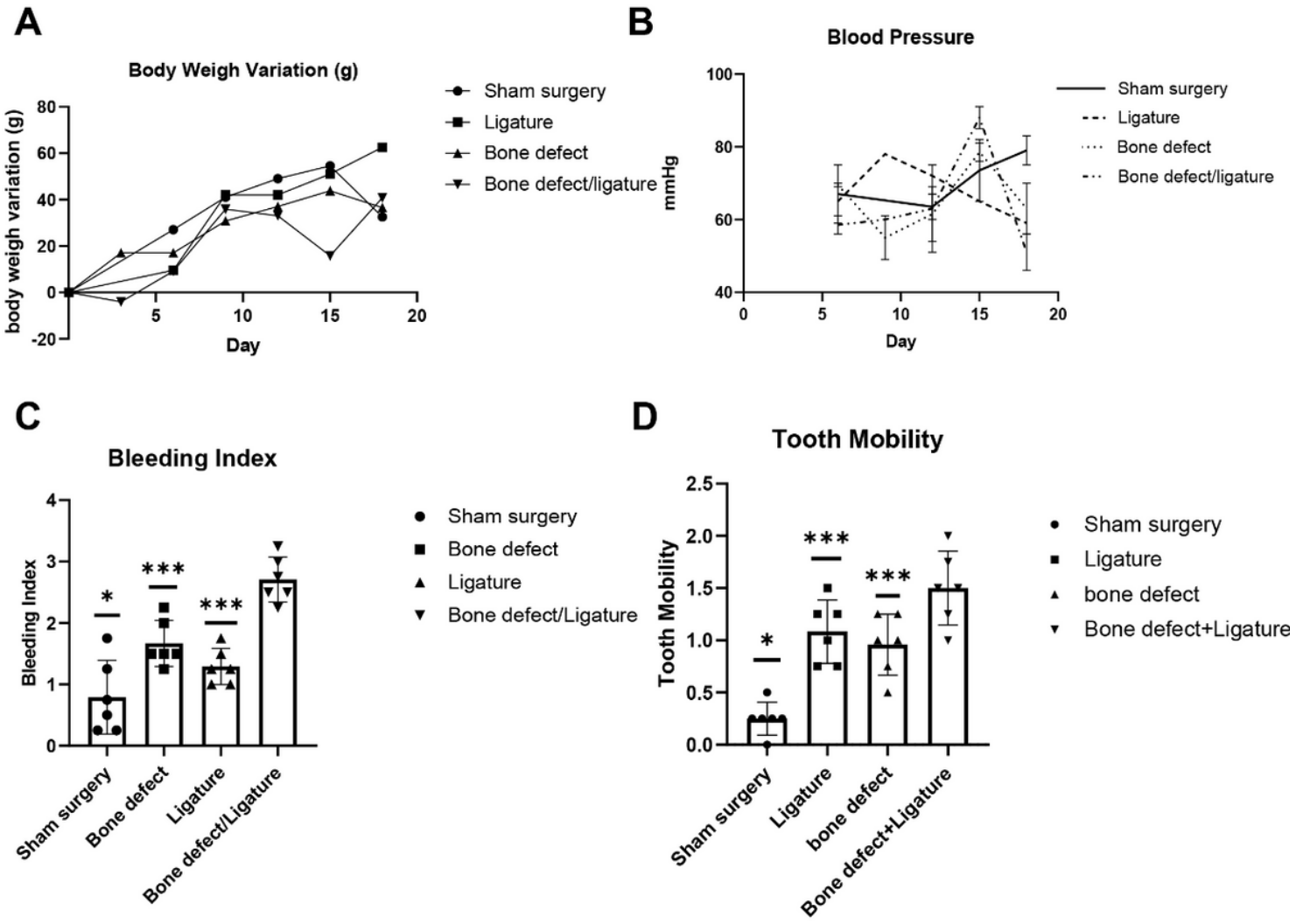

Figure 2

Results of vital signs and clinical indexes of rat periodontitis model A: All animals in the experimental groups presented increase in their weight after the analysis period of 18 days without significant difference. B: no abnormalities were found in blood pressure of all ratsp0.05. C: The mean of BI was significantly higher in bone defect/ligatures compare to the rest three groups. The result of pairwise comparisons of BI were as follows: bone defect/ligature group and bone defect group, p<0.0001; bone defect/ligature group and ligature group, p<0.0001; bone defect/ligature group and sham surgery group, p<0.0001. p<0.0001.*P<0.05**P<0.01 ***P<0.001 D: The mean of TM was significantly higher in bone defect/ligatures compare to the rest three

groups. The result of pairwise comparisons of TM were as follows: bone defect/ligature group and bone defect group, one sample t-test, p<0.005; bone defect/ligature group and ligature group, one sample t-test, p<0.001; bone defect/ligature group and sham surgery group, one sample t-test, p<0.0001.*P<0.05□**P<0.01□***P<0.001. Abbreviations: BI, bleeding index, TM, tooth mobility.

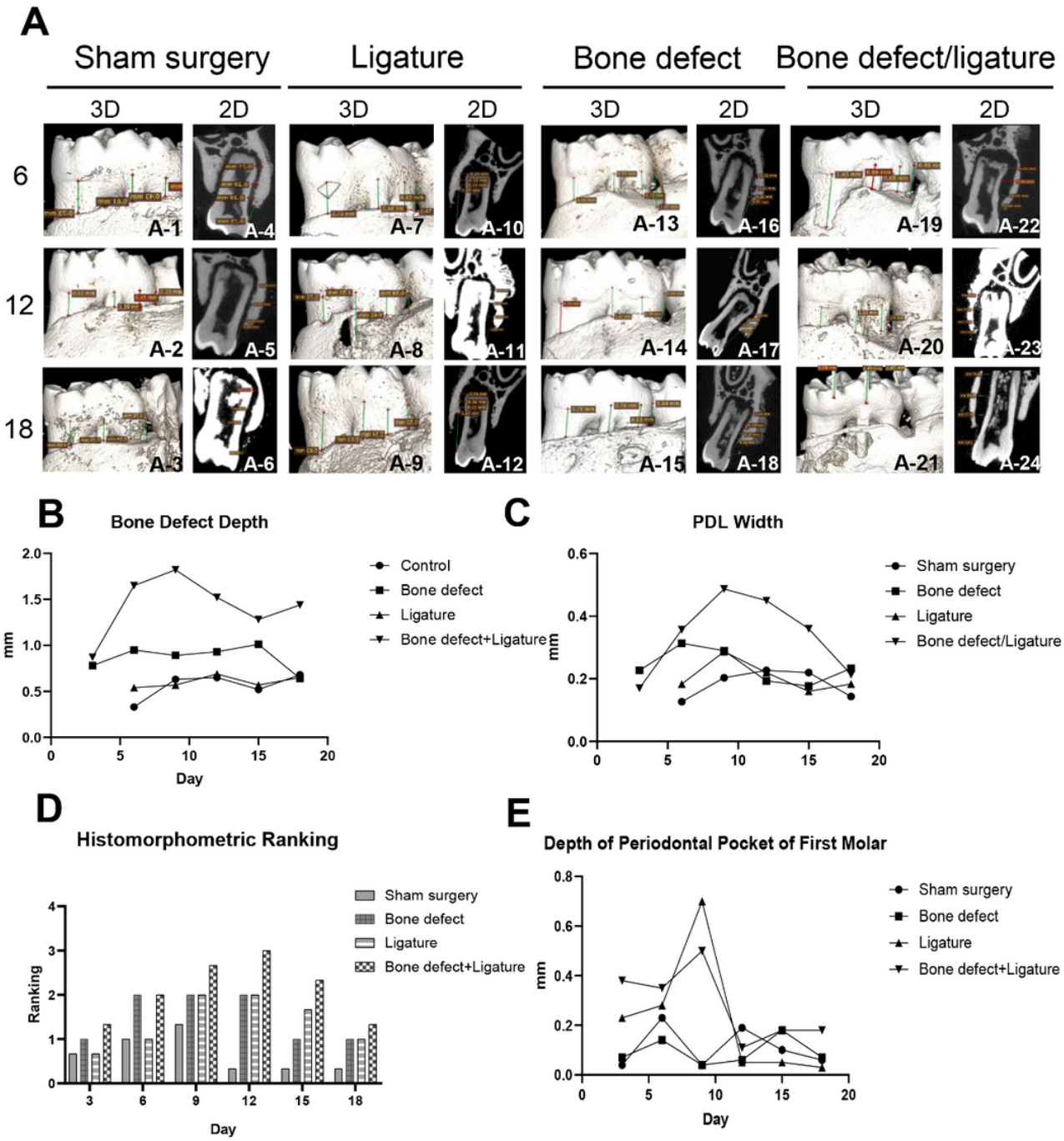

Figure 3

Micro-CT images and histomorphometry of the periapical first molar in rats. A: CT Images of rat periodontitis models. Left (3D reconstructed images): Particularly significant horizontal and vertical bone loss, rough alveolar bone surfaces were observed in the bone defect/ligature group of 6-12 days(A19-20). Smooth surfaces of

alveolar bones were witnessed in the sham surgery group(A-1-3). The surgical defect areas were clear in the bone defect group(A13). Unevenly loss and rough surface of alveolar bones had been observed in the ligature group (A8-9). Right (Two-dimensional micro-CT sections of periodontal ligament width): No significant widening of the periodontal ligament during the 18 days in sham surgery group and bone defect group (A4-6). In ligation group, the periodontium was slightly widened in the early period of 6 day(A10), and gradually returned to the original level afterwards(A11-12). B: bone defect depth measurements of four groups. C: measurements of the periodontal ligament width. D: histomorphometric measurements of PDD of first molar in HE staining sections. E: depth of PDD of first molar by Micro-CT panel sections.

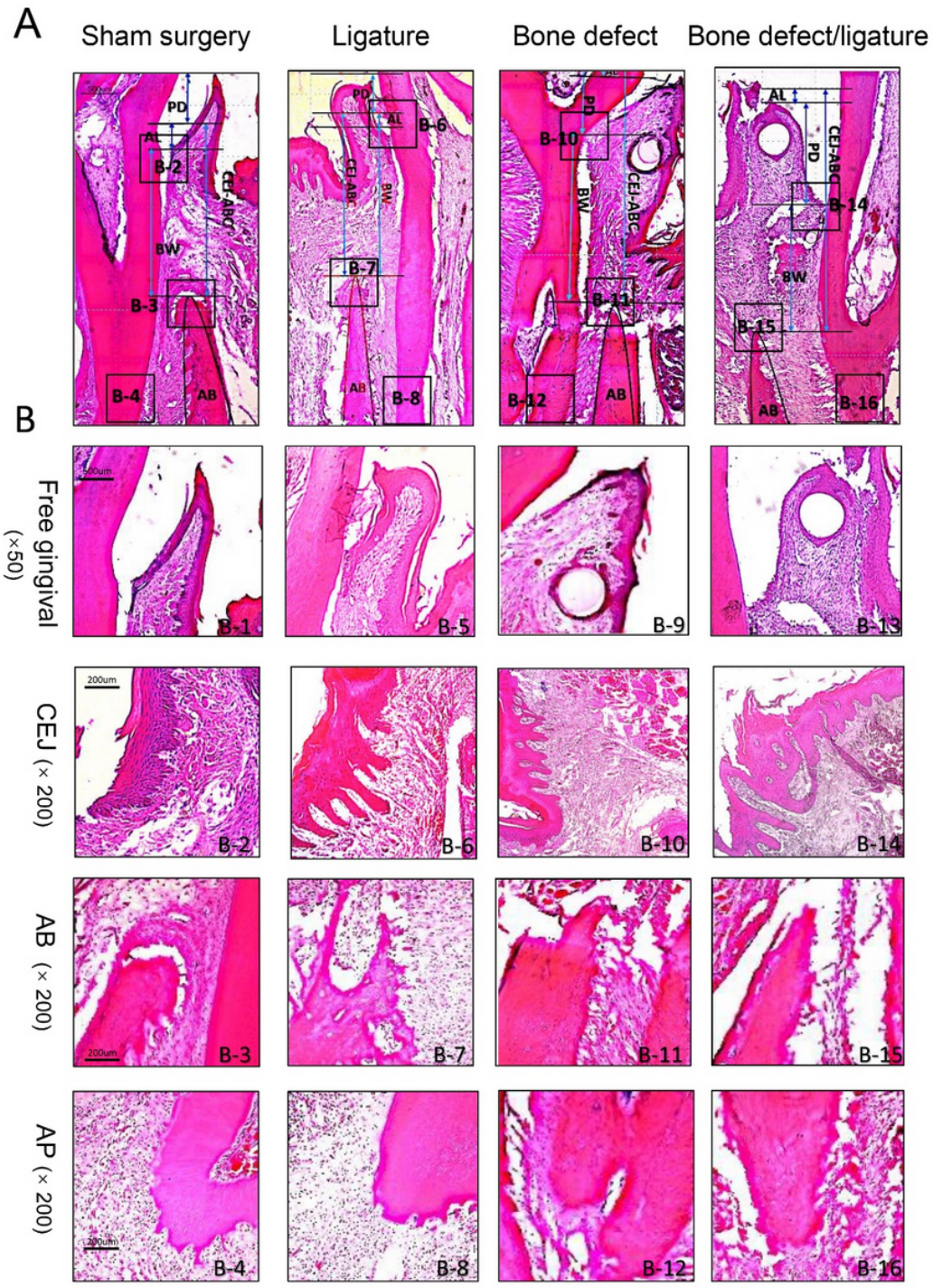

Figure 4

Periodontal tissue and alveolar bone of the distal mesial root of the first molar of rats under light microscopy. (A)Whole view of histopathologic of the distal root of the mandibular first molar by HE staining on Day 9. Measurement of the distance of CEJ-ABC (arrow bars) showing that the attachment loss of junction epithelium in the bone defect/ligature group was longer than that in the other three groups, Scale bar = 100 μm. (B) Free gingiva and junctional epithelium of four groups. Spiky projections were thicker in the bone defect/ligature group (B-14). Ulcer development in the surface of sulcular epithelium, significant infiltration of inflammatory cells, hyperemia and edema of blood vessels, and gingival fibers loss could be observed in the connective tissue in the bone defect/ligature group (B-13-B14). Sucular epithelium was thinner, the epithelium pegs and dermal papillae were shorter and blunter in the sham surgery group (B-2). The rete pegs or ridges and dermal papillae were long and slender in the bone defect group with less infiltration of inflammatory cells underlying in the connective tissue(B-10). Scale bar = 500 μm. Alveolar bone loss in four groups. Prominently horizontal and vertical bone resorption was present in the bone defect/ligature group (B-11), while irregular bone resorption was observed in the ligature group (B-7). Surgical region on the alveolar bone were clearly observed in the bone defect group (B-11). The typical structure of Sharpey's fiber and alveolar bone crest were observed in the sham surgery group (B-3) but could no longer retain in the bone defect/ligature group (B-15). scale bar = 200 μm. Infiltration of inflammatory cells in the apical periodontal ligament. The integrity of cementum and periodontal ligament were lost in the bone defect/ligature group (B-16). Apical periodontal ligament was normal in the sham surgery group without inflammatory invasion (B-4) and partly reserved in the ligature group (B-8) and bone defect group (B-12). scale bar = 200 μm.

Supplementary Files

This is a list of supplementary files associated with this preprint. Click to download.

- Supplemetalmaterial1.tif
- supplementarymaterial2.docx